Theoretical Study of Electron Scattering with NF, NF_2, and NF_3 Molecules

Marwa H. Handhal*, Alaa A. Khalaf

Department of Physics, College of Sciences, University of Basrah, Basra, Iraq

*Corresponding author E-mail: marwa.hameed@uobasrah.edu.iq

https://doi.org/10.29072/basjs.20240209

ARTICLE INFO

Keywords

Electron molecules Collisions, Cross Sections, Scattering, Elastic, Sherman function

ABSTRACT

This article examined the differential cross-section and the integral cross-section (DCS & ICS) for NFx molecules (where x: 1, 2, 3). The molecules underwent electron collisions (elastic scattering) within a defined energy range. A theoretical model has been employed to compute DCS and ICS at specific energies ranging from 1.5 eV to 100 eV. Overall, our DCS findings consistently aligned with measurements from other researchers; however, theoretical investigations on these compounds were limited.

Received 21 Apr 2024; Received in revised form 27 July 2024; Accepted 05 Aug 2024, Published 31 Aug 2024

1. Introduction

A broad spectrum of processes in atoms and molecules is encompassed by electron collision physics. These processes can be comprehended through experimental and theoretical investigations that mutually support and challenge each other [1]. Elastic scattering of electrons is affected meaningfully by their transport through matter [2]. A detailed comprehension of the DCSs for the scattering of electrons is deemed crucial for understanding electron transport, as well as for numerous practical applications [3]. A low-temperature plasma's dynamics are fundamentally influenced by the interactions and collisions between projectiles and targets. When direct observation isn't possible, measurements of emission spectra can provide information about the plasma and its environments [4]. Particles are treated in quantum mechanics as waves, and the probability of a particular scattering process occurring is measured by the amplitude of the wave that is scattering the particle [5].Molecular and nuclear physics are based on an essential concept called differential cross-section, which provides valuable information about the interaction of particles with one another [6]. The scattering probability describes a particular scattering process that is to occur and provides insights into the mechanisms underlying the scattering process [7]. To understand particle interaction, researchers and scientists can measure the DCS to understand the interactions between particles [8]. Many scattering processes and interactions can be studied and compared with theoretical predictions. This allows physicists to test the validity of their theoretical models and refine them as necessary [9]. NF_3 is a colorless gas, that is primarily produced through the reaction of ammonia (NH_3) with fluorine gas (F_2) [10]. It is widely used in various industrial applications. One of its significant uses is as a cleaning agent in the electronics industry. NF_3 is utilized to remove unwanted deposits from the chambers and surfaces of semiconductor manufacturing equipment. It is also employed as a cleaning agent in flat panel displays, solar panels, and other electronic devices [11]. Generally, the theoretical predictions of the total and differential cross-section are compared to experimental measurements to validate or refine the theoretical predictions. Discrepancies between theory and experiment can indicate the need for new physics or improvements in the existing theoretical framework [12]. Also, DCSs and ICS have been presented for NF_2 and NF molecules, but with no comparison for DCS which is unavailable to our knowledge. Experiments and theoretical studies have investigated cross-sections for various electron-NF_3 scattering processes during the past few decades. Szmytkowski et al. [13] conducted a study on the collisions between electrons and nitrogen trifluoride (NF_3)

molecules. This study investigates the total cross sections (TCS) for electron scattering by nitrogen trifluoride. The work by Hamilton et al. [14] examined the electron impact process of NF molecules, specifically NF, NF_2, and NF_3. The authors assert that their anticipated cross-sections for electron collisions with NF_3, NF_2, and NF provide significant insights into plasma dissociation and excitation processes. Goswami et al. [15] showed that the total cross sections (TCS) for electron collisions with NF_3 correspond with theoretical elastic and ionization cross-sections, both qualitatively and quantitatively. The scattering mechanism is elucidated by the independent atom model, which outlines the most basic approach for each atom in a molecule to interact with an ejected electron. Various other methods have been used to obtain metacentric molecular potential. The wave function of the molecule was computed using the Hartree-Fock method. Our main objective is to develop a technique for determining the continuous electron scattering potentials of NF_3 to conduct tests and compare our DCS and TCS with existing comprehensive findings. Given that the wave functions and outgoing potential are provided in an analytical form, we utilized established and extensively validated formulas for calculating energy and the complex optical potential's exchange, polarization, and absorption components.

2. Theoretical Method

The elastic interactions of a projectile with a molecule have a kinetic energy E. When an electron shell has an open configuration, a molecule's electron charge allocation is considered. An optical potential describes the interaction between an electron and a molecule [16],

$$V(r) = V_{st}(r) + V_{ex}(r) + V_{cp}(r) - iW_{abs}(r) \quad (1)$$

$V_{st}(\bar{r})$: interaction potential, $V_{ex}(\bar{r})$: exchange potential, $V_{cp}(\bar{r})$: correlation polarization potential, and $W_{abs}(\bar{r})$: magnitude of the imaginary absorption potential. Due to the assumed spherical symmetry of the atomic charge distribution, the potential (1) and all its components are also spherical. Based on conventional partial-wave methods, elastic-scattering properties can be calculated.

The energy of an electron at a distance (r) from its nucleus is,

$$V_{\mathrm{st}}(r) = Z_0 e\varphi(r) \quad (2)$$

$Z_0 e$: the charge of an electron ($Z_0 = -1$). $\varphi(r)$: the sum of the contributions from the nucleus and the electron cloud in a molecule.

$$\varphi(r) = \varphi_n(r) + \varphi_e(r)$$

$$\varphi_{\mathrm{n}}(r) = e\left(\frac{1}{r}\int_0^r \rho_{\mathrm{n}}(r')4\pi r'^2 \mathrm{d}r' + \int_r^\infty \rho_{\mathrm{n}}(r')4\pi r' \mathrm{d}r'\right), \quad (3)$$

$$\varphi_{\mathrm{e}}(r) = -e\left(\frac{1}{r}\int_0^r \rho_{\mathrm{e}}(r')4\pi r'^2 \mathrm{d}r' + \int_r^\infty \rho_{\mathrm{e}}(r')4\pi r' \mathrm{d}r'\right).$$

We must consider that collisions cause rearrangement of the target, which the electron exchange places with a molecule electron. The best method to deal with electron-exchange effects is to replace the non-local exchange interaction with an approximate local potential. It used the exchange potential that was used before form (Furness & McCarthy) [17], that derived directly from the equation by using a WKB (Wentzel–Kramers–Brillouin) like approximation for the wave functions:

$$V_{ex}{}^{(-)}(\bar{r}) = \frac{1}{2}[E - V_{st}(\bar{r})] - \frac{1}{2}[[E - V_{st}(\bar{r})]^2 + 4\pi a_0 e^4 \rho(r)]^{1/2} \quad (4)$$

The slow electrons polarize the target molecule's charge cloud, resulting in a dipole moment induced on the electron itself. A (Buckingham) potential, applied to the electron backward, can approximate the polarization potential energy when the electron is far from the target.

$$V_{pol}(\bar{r}) = -\frac{\alpha_p e^2}{2(r^2+d^2)^2} \quad (5)$$

α_p: polarizability of the molecule, d: a cutoff parameter, which, polarization potentials at r=0 do not diverge. Following Mittleman and Watson [18], we write

$$d^4 = \frac{1}{2}\alpha_p \alpha_0 Z^{-1/3} b_{pol}^2 \quad (6)$$

b_{pol}: adjustable energy-dependent parameter, $b_{\mathrm{pol}}^2 = max[(E - 50\mathrm{eV})/(16\mathrm{eV}),1]$, Z; atomic number.

Perdew and Zunger's parameterization of electron correlation potentials [25] is adopted,

$V_{\mathrm{co}}^{(-)}(r) = -\frac{e^2}{a_0}(0.0311 \ln r_{\mathrm{s}} - 0.0584 + 0.00133 r_{\mathrm{s}} \ln r_{\mathrm{s}} - 0.0084 r_{\mathrm{s}})$ for $r_{\mathrm{S}} < 1$ and,

$$V_{\mathrm{co}}^{(-)}(r) = -\frac{e^2}{a_0}\beta_0 \frac{1+(7/6)\beta_1 r_s^{1/2}+(4/3)\beta_2 r_s}{\left(1+\beta_1 r_s^{1/2}+\beta_2 r_s\right)^2} \quad \text{for } r_S \geqslant 1 \tag{7}$$

where $\beta_0 = 0.1423, \beta_1 = 1.0529$ and $\beta_2 = 0.3334$. $r_s \equiv \frac{1}{a_0}\left[\frac{3}{4\pi\rho_e(r)}\right]^{\frac{1}{3}}$, is the radius of the sphere that contains one electron of the gas, in units of the Bohr radius a_0.

When projectiles have kinetic energy higher than the threshold for the first excitation, some particles are lost from the elastic channel and go to the inelastic channels. Using a negative imaginary term, $-iWabs(r)$, in the optical model potential allows for the representation of this phenomenon.

$$W_{abs} \equiv \frac{v_L^{(nr)}}{v_L} W_{abs}^{(nr)} = \sqrt{\frac{2(E_L+m_eC^2)^2}{m_eC^2(E_L+2m_eC^2)}} A_{abs}\frac{h}{2}\left[v_L^{(nr)}\rho_e\sigma_{bc}(E_L.\rho_e.\Delta)\right] \tag{8}$$

Where, $v_L^{(nr)}$: Non-relativistic local electron velocity. v_L: relativistic local electron velocity. E_L : Local electron energy. $\rho_e(r)$: Local electron density. Δ:energy gap.

A Dirac equation describes the stationary states of the relativistic particles (electrons) in the potential $V(r)$[19].

$$\mathcal{H}_{\mathrm{D}}\psi(\mathbf{r}) = (E + \mathrm{m_e}c^2)\psi(\mathbf{r}) \tag{9}$$

$$\mathcal{H}_{\mathrm{D}} = c\tilde{\alpha}\cdot\mathbf{p} + \tilde{\beta}\mathrm{m_e}c^2 + V(r) \tag{10}$$

$\psi(\mathbf{r})$: is a wave function. The spherical waves are solutions to the Dirac equation:

$$\psi_{E\kappa m}(\mathbf{r}) = \frac{1}{r}\begin{pmatrix} P_{E\kappa}(r)\Omega_{\kappa,m}(\hat{\mathbf{r}}) \\ \mathrm{i}\ Q_{E\kappa}(r)\Omega_{-\kappa,m}(\hat{\mathbf{r}}) \end{pmatrix} \tag{11}$$

Here *P(r)* & *Q(r)*: the upper and lower component radial functions and the spherical spinors.

$$\begin{aligned} \frac{\mathrm{d}P_{E\kappa}}{\mathrm{d}r} &= -\frac{\kappa}{r}P_{E\kappa} + \frac{E-V+2m_ec^2}{ch}Q_{E\kappa} \\ \frac{\mathrm{d}Q_{E\kappa}}{\mathrm{d}r} &= -\frac{E-V}{ch}P_{E\kappa} + \frac{\kappa}{r}Q_{E\kappa}. \end{aligned} \tag{12}$$

To achieve unit amplitude oscillations for the upper component radial function $P_{E\kappa}(r)$, we must normalize the spherical waves. In $r \to \infty$ and finite range fields, we have:

$$P_{EK}(r) \simeq \sin\left(kr - \ell\frac{\pi}{2} - \eta\ln(2kr) + \Delta + \delta\right) \quad (13)$$

A non-relativistic potential can also cause a phase shift that is positive or negative. This theory applies to electrons as well as positrons; the major difference between them is the sign of their charges, namely, electrons are attracted to atoms and positive ions, while positrons are repelled by them.

Relativistic electron scattering by a real field or complex central field V(r) is completely expressed by the direct and spin-flip scattering amplitudes, given by,

$$f(\theta) = \frac{1}{2ik}\sum_{l=0}^{\infty}\left[(l+1)[\exp(2i\delta_{k=-l-1}) - 1] + l[\exp(2i\delta_{k=l})]\right]P_l(cos\theta) \quad (14)$$

And

$$g(\theta) = \frac{1}{2ik}\sum_{l=0}^{\infty}[exp(2i\delta_{k=l}) - exp(2i\delta_{k=-l-1})]P_l^1(cos\theta) \quad (15)$$

The computer code that is used, delivers the scattering amplitudes and the elastic differential cross-section, and the elastic total cross-section. The differential cross section for elastic scattering of electron beams that are not spin polarized is,

$$\frac{d\sigma}{d\Omega} = |f(\theta)|^2 + |g(\theta)|^2 \quad (16)$$

Also, calculate the total elastic cross-section,

$$\sigma = \int \frac{d\sigma}{d\Omega}d\Omega = \int_0^{\pi}\frac{d\sigma}{d\Omega}2\pi\, sin\theta\, d\theta \quad (17)$$

Spin polarization happens when initially unpolarized beams are scattered by elastic forces. The degree of polarization of electrons scattered in the direction of theta (θ) is given by the Sherman function[20],

$$S(\theta) = i\frac{f(\theta)g^*(\theta) - f^*(\theta)g(\theta)}{|f(\theta)|^2 + |g(\theta)|^2} \quad (18)$$

At specific scattering angles, the absolute value of the Sherman function $S(\theta)$ is close to unity for certain target projectile kinetic energies. Despite their low intensity, elastic scattering constructs highly polarized electron beams under these conditions.

3. Results and discussion

In this work, we calculate the elastic integral and differential cross-section for NF, NF_2, NF_3 molecules interact with electrons beam. But we started with NF_3 first to provide comparisons. The parameters of the target and the principles of coordinate geometry are employed to calculate observable quantities and molecule polarizability. The Hartree atomic units were employed to perform the computations, with h, ħ, and e values of 1. The computed differential cross sections (DCSs) integrated cross sections (ICS), and Sherman functions are typically precise to approximately 0.01% when partial wave analysis is feasible. A presentation and discussion of the computed DCS, TCS, and S(θ) outcomes for both electron and positron scattering are included in the subsequent subsections.

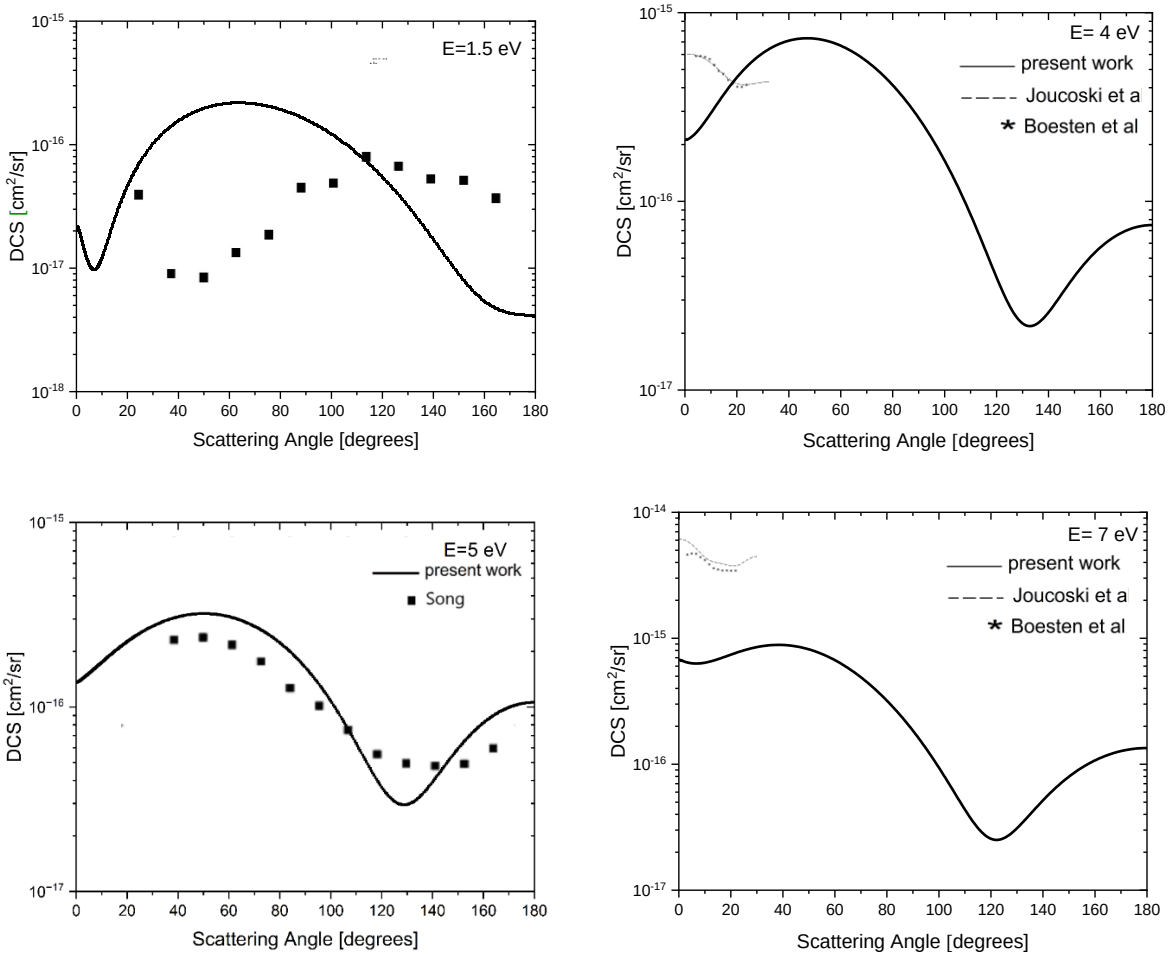

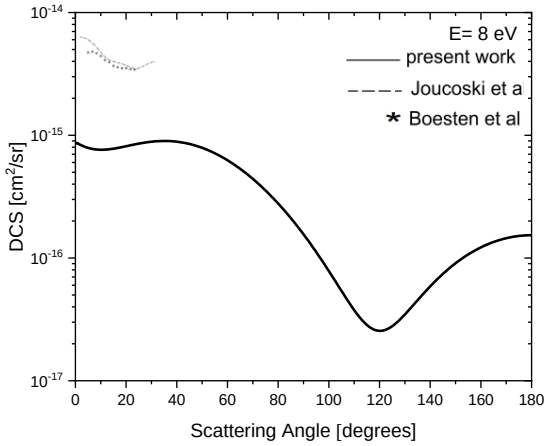

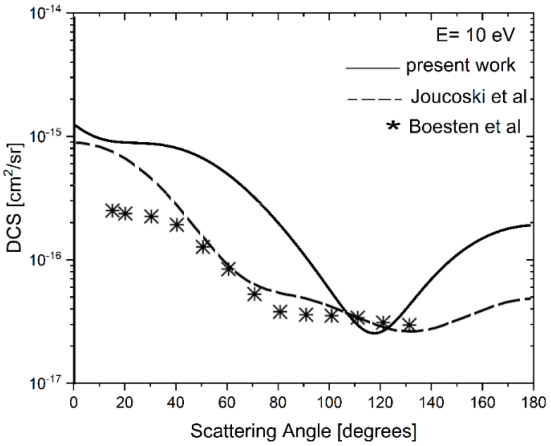

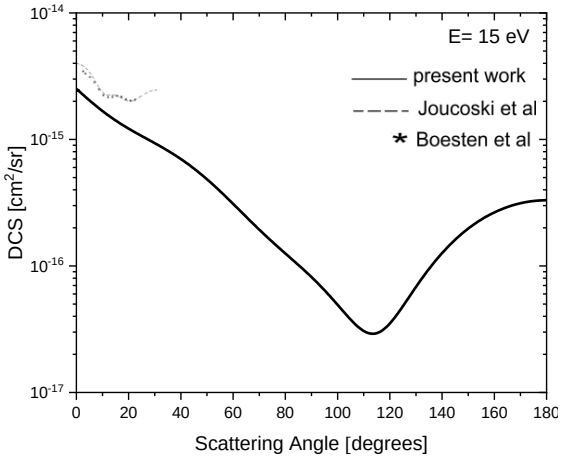

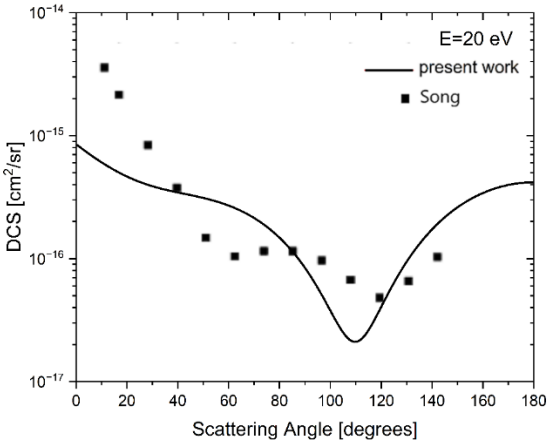

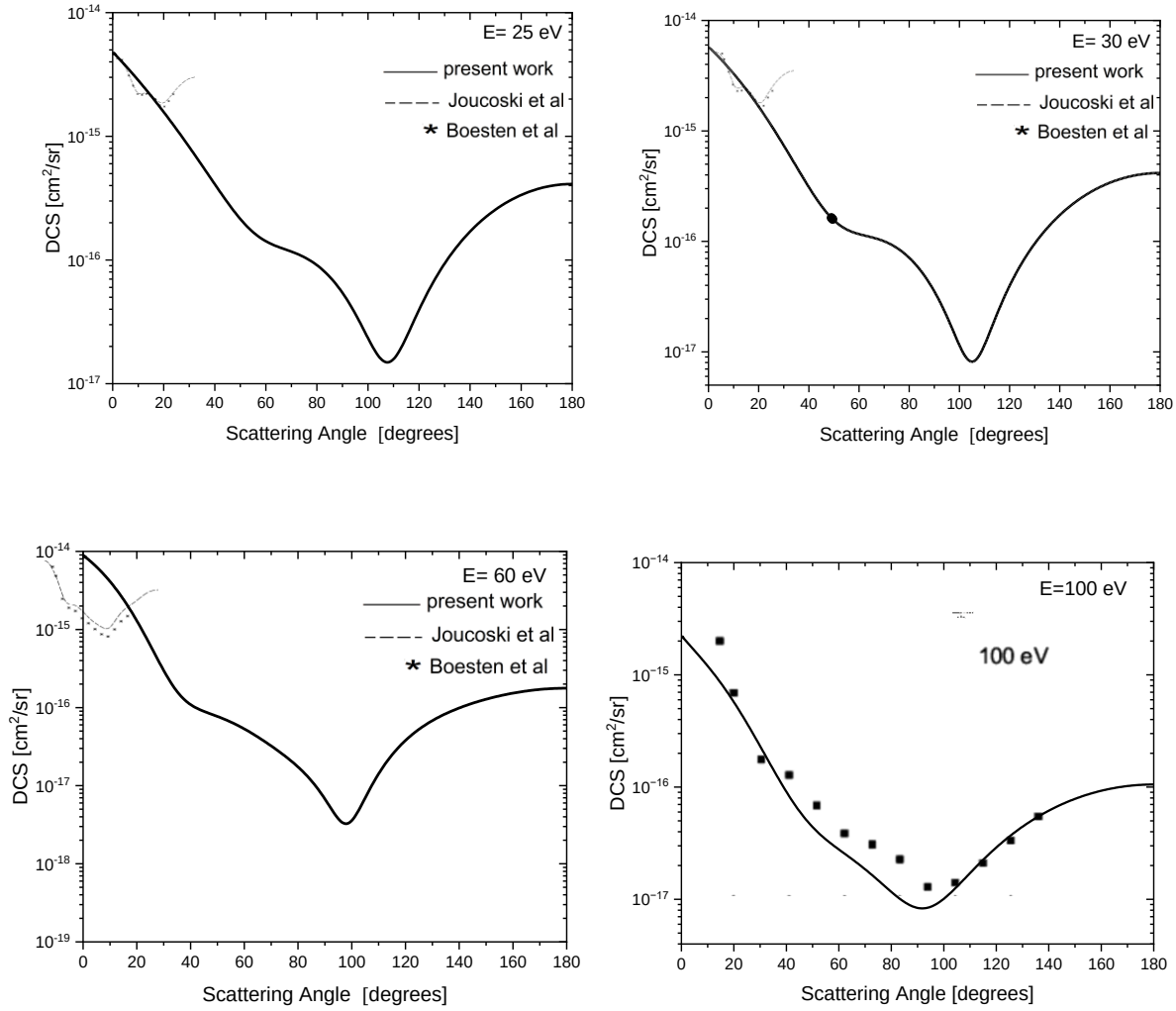

Figure 1: DCS (cm^2/sr) for elastic scattering of electrons with NF_3 at energies (1.5,4,5,7,8,10,15,20,25,30,60,100) eV[21-23]

In Figure 1, a differential cross-section was calculated for many energies for the elastic collision of electrons with NF_3 and compared our results with theoretical data of Joucoski [23] and Boesten [24] for DCSs at (4,7,8,10,15,25,30,60) eV, and the experimental data with Song [21] at (1.5,5,20,100) eV. However, the theoretical data of Differential Cross Sections (DCSs) for low energies agreed reliably with the experimental result. Its data are presented for a specific set of incident electron energies, illustrating the action of the polarization effect, particularly at very low energies, for higher energies at scattering angles less than 80º the behavior of DCS takes the maximum values due to incident electrons approaching straight or obtuse angles. Backscattering is also responsible for values above 100º.

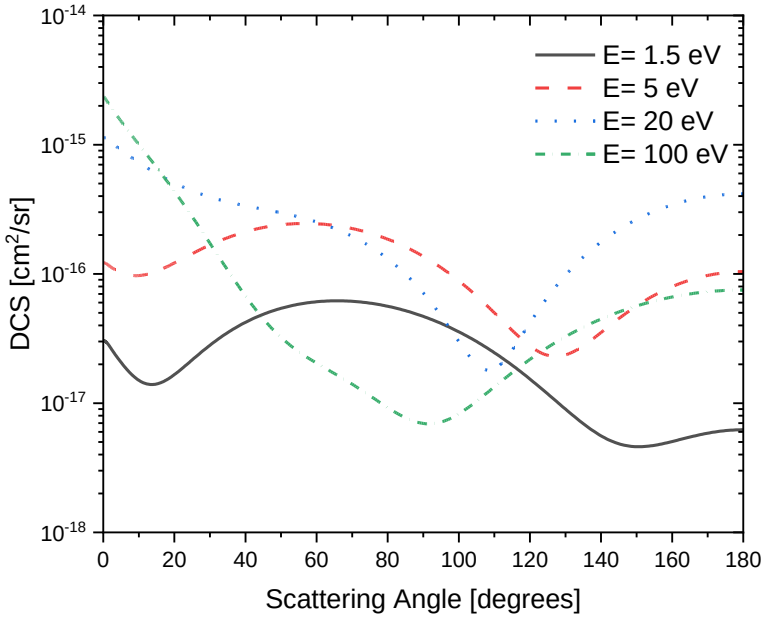

Figure 2: DCS (cm^2/sr) for elastic scattering of electrons with NF_2 at energies (1.5,5,20,100) eV

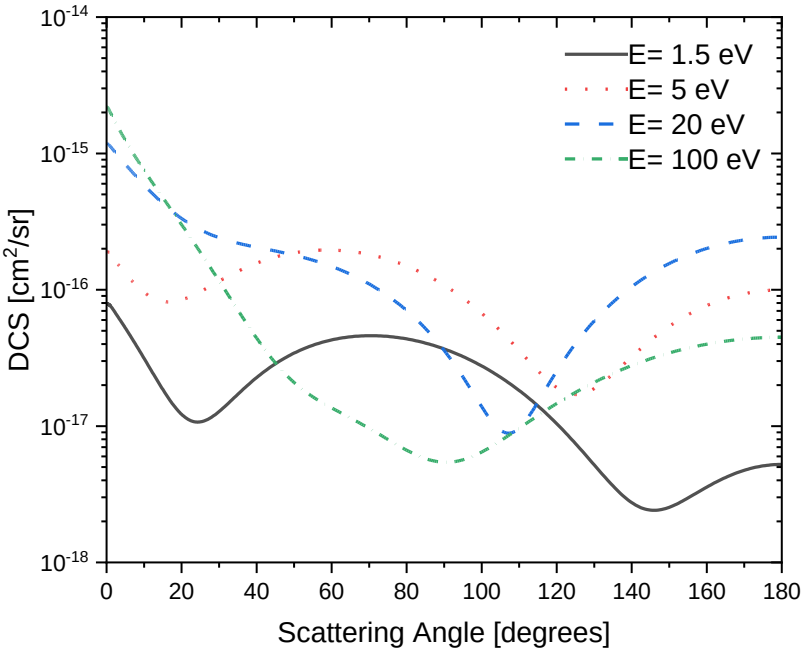

Figure 3: DCS (cm^2/sr) for elastic scattering of electrons with NF at energies (1.5,5,20,100) eV

In figures 2 &3, we presented our data for various energies representing for DCS of NF_2 and NF molecules. Clear in these figures is the impact of scattering and backscattering, particularly at higher energy levels. It should be noted, however, that DCS values for indirect scattering remain quite lower than those for direct scattering since the molecules structure of the (NF, NF_2) molecules is quite different from that of the NF_3. In lower energies, the DCS values do not show the same behavior that they exhibit at higher energies. To comprehend the reasons behind this difference in DCS behavior at low energies, an examination of the molecule's properties and the potential energy of the system is necessary. There might be an influence of these factors on the interaction between an electron and the NF_2 molecule within a specific energy range.

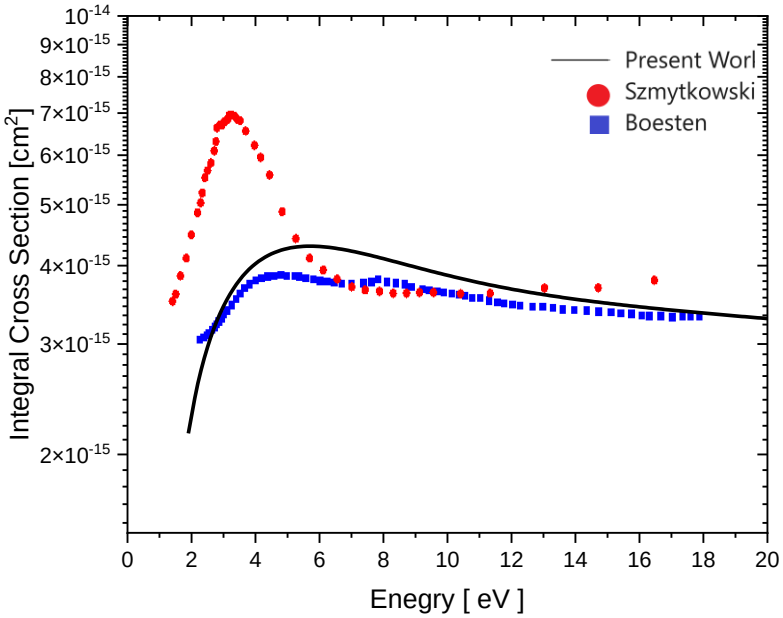

Figure 4: Elastic integral cross section for NF_3 at a range of low energies, compared with, Szmytkowski [24], Boesten [24],the black line is my present work.

Figure 4 shows the integral cross section for NF_3 results are discussed and compared to experimental data Szmytkowski [20], Song [21], Boesten [24].

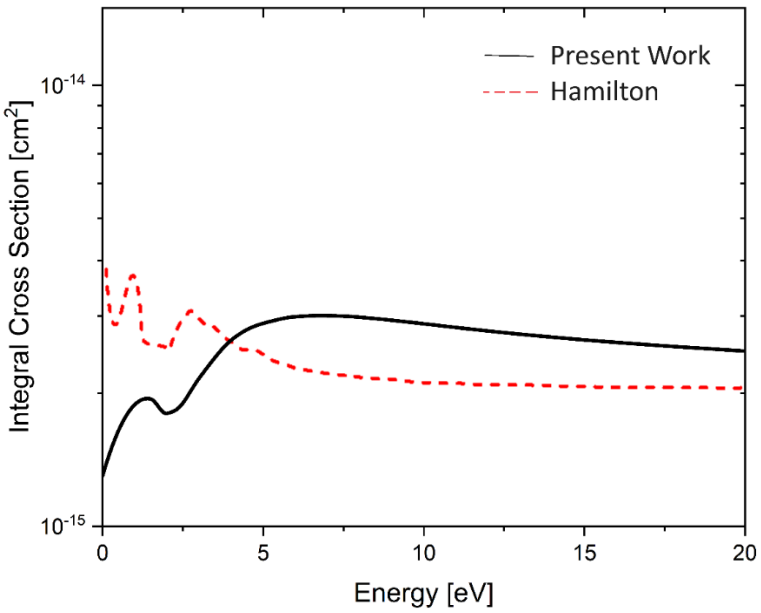

Figure 5: Elastic integral cross section for NF_2 at a range of low energies, compared with Hamilton [26]

Figure 5 shows the integral cross section for NF_2 results discussed and compared to theoretical data Hamilton [26].

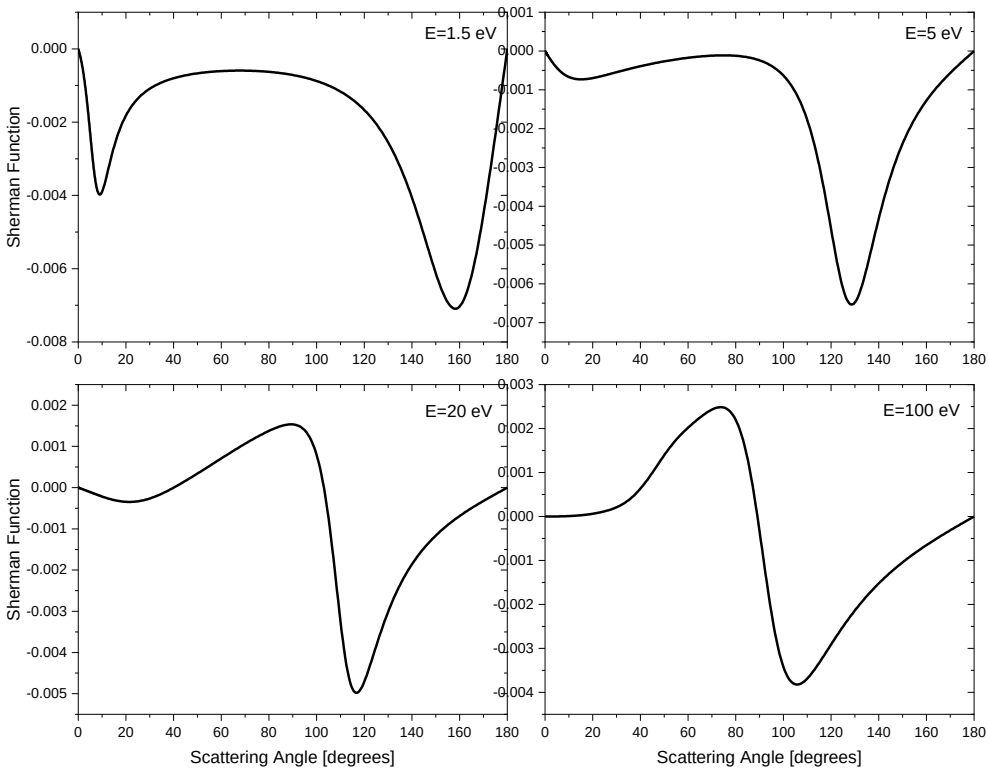

Figure 6: S(θ), for the e^- -NF_3 elastic scattering calculated in this study at the energies (1.5 eV;5 eV;20 eV;100 eV)

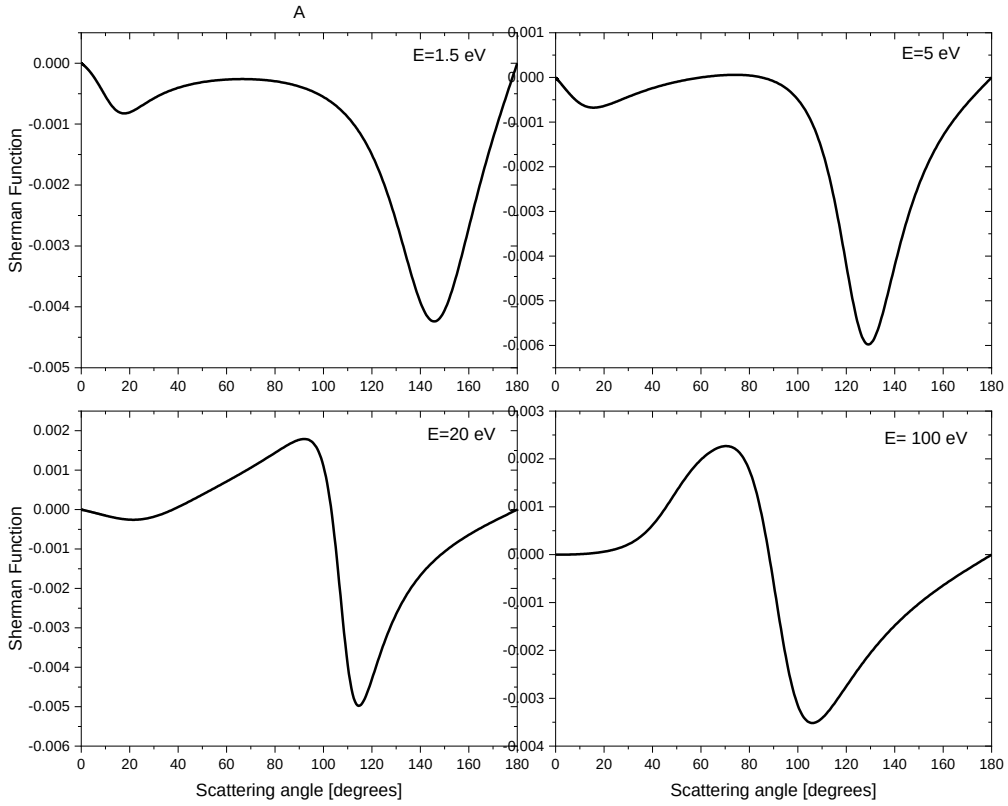

Figure 7: S(θ), for the e^- -NF_2 elastic scattering calculated in this study at the energies (1.5 eV;5 eV;20 eV;100 eV)

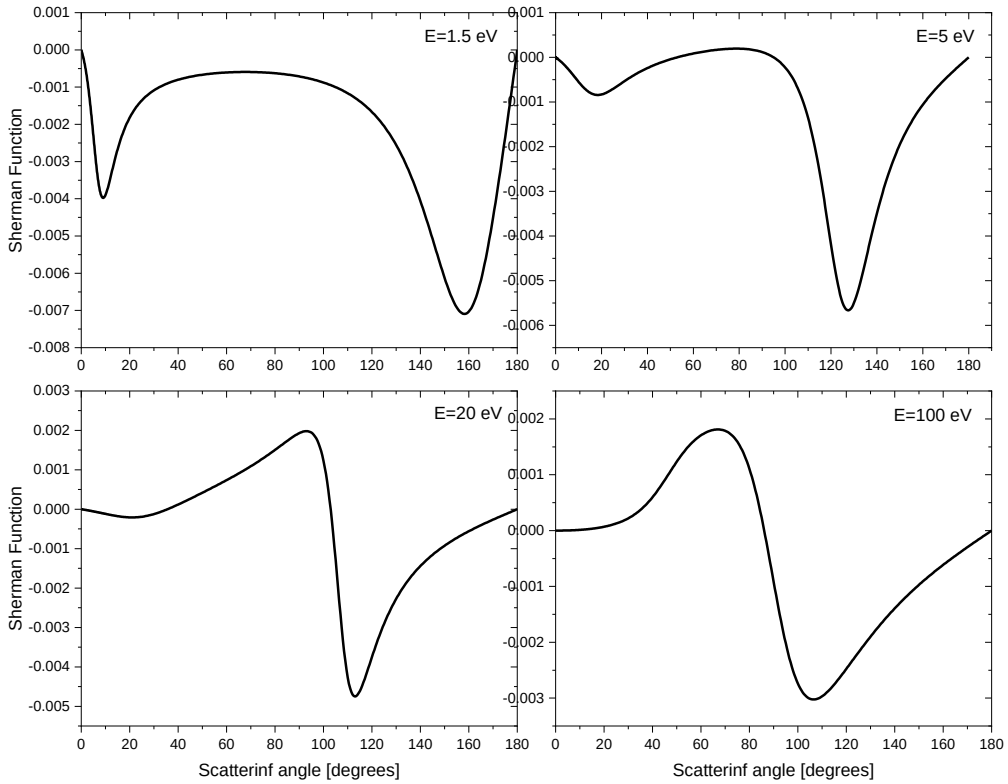

Figure 8: S(θ), for the e^- -NF elastic scattering calculated in this study at the energies (1.5 eV;5 eV;20 eV;100 eV*)*

The Sherman function, as shown in Figures (6,7,8), demonstrates a correlation between its behaviors and the scattering angle. This is because polarized spin electrons transition from an upward to a downward direction when the current is flowing. When the angle is large, the polarization value becomes negative. Resonances allow the polarization value of (NF, NF_2, NF_3) to become positive at energies ranging from 20 to 100 eV when observed at low angles. The peaks of Sherman are more prominent for higher energies. The attribution of these behaviors to either the structural effect or the target distortion needs to be clarified. At low energies (1.5,5) eV, the behaviors of the Sherman function are altered. This is attributed to the diminishing sensitivity as the size of the other phase shifts progressively rises with increasing energy. However, the method seems applicable at energies of up to around 5 electron volts (eV).

4. Conclusions

This article studies three molecules (NF, NF_2, NF_3) and discusses the elastic integral and differential cross-section for those molecules, as greenhouse gases they affect the environment and global warming, and spin polarization for the electron impact scattering from (NF, NF_2, NF_3) molecules over a wide range of incident energy of ($1\ eV \leq Ei \leq 100\ eV$) and scattering angles of ($0^\circ \leq \theta \leq 180^\circ$). All the above scattering observables were calculated within the framework of Dirac partial wave analysis. were compared with the available experimental results and other theoretical results that were obtained by using different methods and potentials. The comparison shows that our results reasonably agree with the available experimental measurements and other theoretical findings.

References

[1] R.M.A. Hassan, A.A. Khalaf, Atomic Lithium Excitation by Electron Impact, Journal of Kufa-Physics, 11 (2019) 29-33. http://dx.doi.org/10.31257/2018/JKP/2019/110205

[2] B.C. Saha, D. Jakubassa-Amundsen, A. Basak, A. Haque, M. Haque, M.H. Khandker, M.A. Uddin, Elastic scattering of electrons and positrons from alkali atoms, Adv Quantum Chem, 86(2022)1-149, https://doi.org/10.1016/bs.aiq.2021.08.002

[3] R.A. Boadle, Fundamental studies of positron scattering from atoms and molecules, Thesis, 2018, https://doi.org/ 10.25911/5C6E70B6F1F0C

[4] S. Wilczek, J. Schulze, R.P. Brinkmann, Z. Donkó, J. Trieschmann, T. Mussenbrock, Electron dynamics in low pressure capacitively coupled radio frequency discharges, J Appl Phys, 127 (2020) 181101, https://doi.org/10.1063/5.0003114

[5] D. Belkic, Principles of quantum scattering theory, CRC Press, 2020, https://doi.org/10.1201/9780429146497

[6] A. Belyaev, D.A. Ross, The basics of nuclear and particle physics, Springer, 2021. https://doi:10.1007/978-3-030-80116-8

[7] B. Jiang, J. Li, H. Guo, High-fidelity potential energy surfaces for gas-phase and gas–surface scattering processes from machine learning, J Phys Chem Lett, 11 (2020) 5120-5131, https://doi.org/10.1021/acs.jpclett.0c00989

[8] J. Silberstein, A Toy Model for Dark Photon Compton Scattering, The College of William and Mary, 2020.

[9] A.K. Yassir, A.A. Khalaf, Electron collision with Ammonia and phosphine at wide range of energies, Journal of Kufa-Physics, 14 (2022) 59-74, http://dx.doi.org/10.31257/2018/JKP/2022/140208

[10] B.K. Sovacool, S. Griffiths, J. Kim, M. Bazilian, Climate change and industrial F-gases: A critical and systematic review of developments, sociotechnical systems and policy options for reducing synthetic greenhouse gas emissions, Renew. Sustain. Energy Rev., 141 (2021) 110759, https://doi.org/10.1016/j.rser.2021.110759

[11] S. An, S.J. Hong, Spectroscopic Analysis of NF3 Plasmas with Oxygen Additive for PECVD Chamber Cleaning, Coatings, 13 (2023) 91, https://doi.org/10.3390/coatings13010091

[12] D. Neudecker, O. Cabellos, A.R. Clark, M.J. Grosskopf, W. Haeck, M.W. Herman, J. Hutchinson, T. Kawano, A.E. Lovell, I. Stetcu, Informing nuclear physics via machine learning methods with differential and integral experiments, Phys Rev C, 104 (2021) 034611, https://doi.org/10.1103/PhysRevC.104.034611

[13] C. Szmytkowski, A. Domaracka, P. Możejko, E. Ptasińska-Denga, Ł. Kłosowski, M. Piotrowicz, G. Kasperski, Electron collisions with nitrogen trifluoride (NF 3) molecules, Phys Rev A, 70 (2004) 032707, https://doi.org/10.1103/PhysRevA.70.032707

[14] J.R. Hamilton, J. Tennyson, S. Huang, M.J. Kushner, Calculated cross sections for electron collisions with NF3, NF2 and NF with applications to remote plasma sources, Plasma Sources Sci T, 26 (2017) 065010, http://doi.org/10.1088/1361-6595/aa6bdf

[15] B. Goswami, R. Naghma, B. Antony, Cross sections for electron collisions with NF 3, PHYS REV A, 88 (2013) 032707. https://doi.org/10.1103/PhysRevA.88.032707

[16] F. Salvat, A. Jablonski, C.J. Powell, ELSEPA—Dirac partial-wave calculation of elastic scattering of electrons and positrons by atoms, positive ions and molecules, Comput Phys Commun, 165 (2005) 157-190, https://doi.org/10.1016/j.cpc.2004.09.006

[17] J. Furness, I. McCarthy, Semiphenomenological optical model for electron scattering on atoms, J Phys B-At Mol Opt, 6 (1973) 2280, http://doi.org/10.1088/0022-3700/6/11/021

[18] M.H. Mittleman, K.M. Watson, Effects of the Pauli principle on the scattering of high-energy electrons by atoms, Ann Phys-New York, 10 (1960) 268-279, https://doi.org/10.1016/0003-4916(60)90024-5

[19] F. Salvat, A. Jablonski, C.J. Powell, elsepa—Dirac partial-wave calculation of elastic scattering of electrons and positrons by atoms, positive ions and molecules (New Version Announcement), Comput Phys Commun, 261 (2021) 107704, https://doi.org/10.1016/j.cpc.2020.107704

[20] D. Jakubassa-Amundsen, R. Barday, The Sherman function in highly relativistic elastic electron–atom scattering, J Phys G Nucl Partic, 39 (2012) 025102, http://doi.org/10.1088/0954-3899/39/2/025102

[21] M.-Y. Song, J.-S. Yoon, H. Cho, G.P. Karwasz, V. Kokoouline, Y. Nakamura, J.R. Hamilton, J. Tennyson, Cross sections for electron collisions with NF3, J Phys Chem Ref Data, 46 (2017) 043104, https://doi.org/10.1063/1.5000687

[22] E. Joucoski, M. Bettega, Elastic scattering of low-energy electrons by NF3, J PHYS B-AT MOL OPT, 35 (2002) 783, http://doi.org/10.1088/0953-4075/35/4/303

[23] B. Goswami, R. Naghma, B. Antony, Cross sections for electron collisions with NF 3, Phys Rev A, 88 (2013) 032707. https://doi.org/10.1103/PhysRevA.88.032707

[24] C. Szmytkowski, A. Domaracka, P. Możejko, E. Ptasińska-Denga, Ł. Kłosowski, M. Piotrowicz, G. Kasperski, Electron collisions with nitrogen trifluoride (NF 3) molecules, Phys Rev. A, 70 (2004) 032707, https://doi.org/10.1103/PhysRevA.70.032707

دراسة نظرية لاستطارة الالكترون مع جزيئات NF NF_3, NF_2

مروة حميد حنظل علاء عبد الحسن خلف

قسم الفيزياء، كلية العلوم، جامعة البصرة، البصرة، العراق

المستخلص

تناول هذا المقال المقطع العرضي التفاضلي DCS والمقطع العرضي الكلي ICS لجزيئات NFx (حيث x: 1، 2، 3). تعرضت الجزيئات لاصطدامات الإلكترونات (التشتت المرن) ضمن نطاق طاقة محدد. تم استخدام نموذج نظري لحساب DCS وICS في طاقات معينة تتراوح بين 1.5 إلكترون فولت إلى 100 إلكترون فولت. بشكل عام، كانت بياناتنا لـ DCS متفقة بشكل موثوق مع تلك التي قام بها الباحثون الآخرون، في حين كانت الدراسات النظرية لهذه الجزيئات قليلة جدًا.